Applied Energy 115 (2014) 559–572

Contents lists available at ScienceDirect

Applied Energy

journal homepage: www.elsevier.com/locate/apenergy

Comparative and sensitive analysis for parabolic trough solar collectors with a detailed Monte Carlo ray-tracing optical model

Z.D. Cheng, Y.L. He *, F.Q. Cui, B.C. Du, Z.J. Zheng, Y. Xu

Key Laboratory of Thermo-Fluid Science and Engineering of MOE, School of Energy and Power Engineering, Xi'an Jiaotong University, Xi'an, Shaanxi 710049, China

HIGHLIGHTS

- It is to present comparative and sensitive analysis for PTCs with the MCRT method.
- A detailed PTC optical model was developed based on a novel unified MCRT model.
- Reference data determined by the divergence effect is useful to design a better PTC.
- Different PTCs have different levels of sensitivity to different optical errors.
- There are no contradictions between accuracy requirements of different parameters.

ARTICLE INFO

Article history:
Received 29 July 2013
Received in revised form 31 October 2013
Accepted 1 November 2013
Available online 4 December 2013

Keywords:
Parabolic trough solar collector
Monte Carlo ray-tracing
Comparative analysis
Geometric parameter
Sensitive analysis

ABSTRACT

This paper presents the numerical results of the comparative and sensitive analysis for different parabolic trough solar collector (PTC) systems under different operating conditions, expecting to optimize the PTC system of better comprehensive characteristics and optical performance or to evaluate the accuracy required for future constructions. A more detailed optical model was developed from a previously proposed unified Monte Carlo ray-tracing (MCRT) model. Numerical results were compared with the reference data and good agreements were obtained, proving that the model and the numerical results are reliable. Then the comparative and sensitive analyses for different PTC systems or different geometric parameters under different possible operating conditions were carried out by this detailed optical model. From the numerical results it is revealed that the ideal comprehensive characteristics and optical performance of the PTC systems are very different from some critical points determined by the divergence phenomenon of the non-parallel solar beam, which can also be well explained by the theoretical analysis results. For different operating conditions, the PTC systems of different geometric parameters have different levels of sensitivity to different optical errors, but the optical accuracy requirements from different geometric parameters of the whole PTC system are always consistent.

1. Introduction

The carbon dioxide induced global warming or climate change has become a pressing issue for years, due to the rapidly increasing energy demand and growing environmental degradation of burning fossil fuel [1–4]. Efficient utilization of renewable energy resources, especially solar energy, is increasingly being considered as a promising solution to this problem [1]. Compared with numerous techniques for solar energy utilizations, the parabolic trough solar collector (PTC) technology in concentrating solar power (CSP) systems is the most mature and widespread technology for the exploitation of solar energy on a large scale [5–7]. However, though the PTC CSP technology has the lowest cost among solar power systems, the cost is still more expensive than that of the conventional fossil fuel power plants. To achieve electricity generation cost that is competitive to fossil power plants, further developments of the solar components with regard to cost reductions and performance improvements are necessary, especially for solar collectors [8].

The PTC system uses mirrored surfaces of a linear parabolic reflector to focus direct solar radiation onto a tubular solar receiver. The receiver is positioned along the focal line of the parabola, and it mainly consists of an absorber tube and a glass cover. The concentrated solar radiation is absorbed and converted into thermal energy by the heat transfer fluid (HTF) flowing through the absorber tube, while the protecting evacuated glass cover is used to reduce the convection heat loss from the absorber [4,7,9–11]. The whole process of the photo-thermal conversion in the PTC system is very complex, since it includes the physical process of photon energy concentrating, collecting, converting, and coupling nonuniform heat transfers with nonuniform fluid dynamics [12,13].

* Corresponding author. Tel.: +86 029 82665930; fax: +86 029 82665445.
E-mail address: yalinghe@mail.xjtu.edu.cn (Y.L. He).

0306-2619/$ - see front matter © 2013 Elsevier Ltd. All rights reserved.
http://dx.doi.org/10.1016/j.apenergy.2013.11.001

Nomenclature

a	the aperture width (m)
d_a	outer diameter of absorber tube (m)
d_g	outer diameter of glass cover (m)
d_{min}	the width of the focal shape (m)
f	the focal length (m)
L_r	active receiver length (m)
N_c	grid number at the absorber surface
N_o	the ideal surface normal direction
N_s	the actual surface normal direction
q_{ave}	average solar energy flux density (W m^{-2})
q_i	local solar energy flux density (W m^{-2})
q_{max}	maximal solar flux density (W m^{-2})
$q_{SR,i}$	local solar flux density of the ith grid (W m^{-2})
$q_{SR,in}$	total incident solar radiation (kW)
$q_{u,ab}$	absorbed solar energy (kW)

Greek symbols

α_a	absorptivity of the absorber
δ	finite size of the sun (δ = 16′ or 0.465 mrad)
φ_m	the rim angle (°)
η_o	the optical efficiency
ρ_r	reflectivity of the reflector
σ_q	nonuniformity of solar flux density distribution
σ_s	surface error (mrad)
σ_t	tracking error (mrad)
τ_g	transmissivity of the glass cover

Many significant studies on the optical and/or thermal performance of this process have been carried out, especially for the receiver heat loss testing and modeling [14–35]. The heat loss of different receivers are relatively easy to be determined and compared by some common modes from the energy balance in door (with electrical heating) or outdoor (with concentrated solar radiation), such as the steady state equilibrium, the quasi-steady-state equilibrium and the glass tube surface temperature measurements [34–37]. Unlike a separated receiver, the optical performance of the reflector and the corresponding overall thermal performance of the whole PTC system vary substantially with random optical errors and the weather or operating conditions. Therefore, comparative experiments for different linear parabolic optical systems cannot be easily performed through rigorous tests on the installed concentrators and the conditions expected in service. In this case, concentrating solar thermal researches may heavily rely on the numerical analysis to optimize solar concentrators or to provide radiative boundary conditions for the receiver modeling [38]. Thus, a validated accurate PTC optical model can be a powerful instrument for the efficiency analysis of the PTC system [6].

There are many published optical models developed to quickly predict the concentrated solar flux distributions or the optical performance of PTCs. They usually are based on the simple geometric analytical methods or the integral methods early [39–49]. The sunshape, the surface contour and the sun tracking can be simply considered in these analyses. But in order to accurately study the optical effects, a ray-tracing analysis is required [6]. Among numerous significant studies [50], Grena [6] developed a useful PTC optical model recently, using a three-dimensional ray-tracing technique. The model treats the PTC system as translation symmetry and the results are only referred to a section of the receiver, which may not present accurate comprehensive characteristics and optical performance under various realistic operating conditions. Over the years, the Monte Carlo ray-tracing (MCRT) method has been proven to be a more flexible and efficient numerical method to simulate the concentrating characteristics of solar collectors [12,21,50–57]. Many significant numerical PTC models based on this method have been developed in recent years, which have been thoroughly tested or experimentally validated. Some of them are optical models for calculations of concentrated solar flux distributions [27,38,58]. Some are thermal models for simulations of the coupled heat transfer process in the PTC systems, which are performed by combining the MCRT method with the Finite Element Method (FEM) [23,24,53] or the Finite Volume Method (FVM) [9,28,59–62]. In the meantime, the authors also developed an optical and thermal model for the PTC system with the MCRT method [21,22,25,26]. Very recently, to develop a general-purpose numerical tool for typical concentrating solar collectors of CSP systems, a novel unified MCRT code has been further proposed and used [56]. However, to the best of our knowledge, few comprehensive studies have been found in the literatures on comparative analysis for typical PTC systems available and optical sensitivity studies on effects of main geometric parameters under real operating conditions, such as the realistic sun-shape profile, optical properties, non-orthogonal incidence, tracking errors, and imperfect mirror surface. Since a thorough knowledge of diverse effects on the PTC performance characteristics is urgently needed so that high performance PTCs can be obtained. Therefore, a more detailed optical model, based on the previously proposed unified MCRT modeling design and unified solving methods [56], is further developed and used in this paper, expecting to optimize the PTC system of better comprehensive characteristics and optical performance or to evaluate the accuracy required for future constructions.

2. Model and methodology description

2.1. Physical model

A schematic diagram of a cross-section of a PTC system is shown in Fig. 1(a). In the reference system used here, the Y–Z plane contains the parabolic section, with the vertex and the focus at $y = 0$ plane, and the X axis lies on the vertex line of the parabolic mirror. From the diagram, it can be seen that the PTC module mainly includes a parabolic trough reflector and an evacuated tubular receiver. Some important parameters are also presented detailedly, such as the focal length (f), the aperture width (a), the rim angle (φ_m), the absorber diameter (d_a), the glass cover diameter (d_g), the light cone (δ indicates the divergence phenomenon of the non-parallel solar beam caused by the effect of the finite size of the sun), and some typical optical errors. Since the optical errors always enlarge the image of the concentrated solar radiation and reduce the optical performance of the PTC system, it is necessary to know the effects of these optical errors on the reflected rays and the optical performance [52,63]. The optical errors mainly include the surface imperfections/errors (σ_s) and tracking errors (σ_t). For real surfaces, there are four classes of surface imperfections, including the nonspecularity error, the slope error, the shape error and the alignment/installation error [58]. The imperfections are quantified by considering the angular deviation between the actual (N_s) and ideal (N_o) surface normal directions, or between the ideal specular and deviant reflection directions. It is generally assumed that all surface errors can be introduced by the Gaussian distribu-

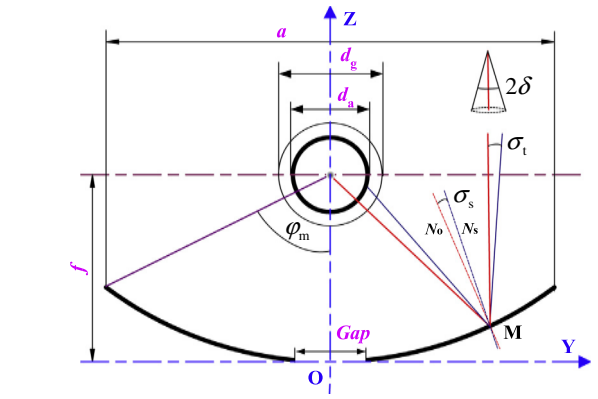

(a) Schematic of a cross-section of a parabolic trough solar collector

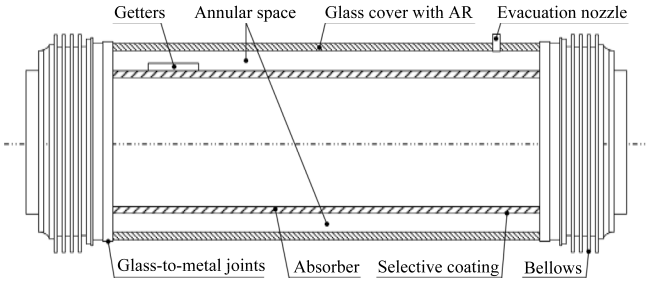

(b) Schematic of the evacuated tubular receiver

Fig. 1. Schematic of the physical model of a parabolic trough solar collector system.

tion [52,58]. For tracking mirrors, an additional tracking error exists. It is the angle error in pointing the collector towards the sun. In addition, to support the receiver located along the focal line of the parabola, a small gap (*Gap*) between two halves of the reflector are given to install the flange or support the bracket. It also reduces the cost of the reflector manufacture without losing efficiency, since the receiver always shadows this area. In this paper, the effects of the small gap are also taken into account while other mirror surfaces are assumed continuous.

A detailed schematic diagram of the evacuated tubular receiver is presented in Fig. 1(b). It can be seen that the receiver mainly includes an inner stainless steel absorber tube with a solar-selective absorbing coating on its outer surface, an outer glass cover with anti-reflective (AR) coatings on its both surfaces, an annular vacuum space, the getters, the bellows and the glass-to-metal joints at its ends, etc. The absorbing coating is sputtered onto the absorber tube to result in excellent selective optical properties, i.e., a high solar absorptance of solar radiation and a low thermal emissivity, to reduce thermal reradiation from the absorber tube to the glass cover [16]. The glass cover is used to reduce heat loss while the AR coatings on its both surfaces are used to reduce Fresnel reflective losses [4,7]. The annular space between the absorber tube and the glass cover is vacuumed to significantly reduce convection heat loss and protect the coatings from oxidation. The vacuum is typically maintained at about 0.0001 torr determined by the Knudsen gas conduction range [10,12]. The getters are installed in the vacuum space to absorb gas molecules that permeate into the annulus over time and indicate status of vacuum, while the vacuum-tight enclosure is sealed by glass-to-metal joints at both ends with bellows that accommodate for thermal expansion difference between steel and glass materials [7,60]. Since they are always protected by shields, the bellows and glass-to-metal joints as well as structure elements (the support rods and the shielding of receiver joints) are not taken into account in the optical model. That is, only the active aperture length of the reflector and the receiver is studied here.

2.2. Detailed MCRT model

The MCRT optical model is a powerful tool for simulating the concentrating characteristics of PTCs. Its methodology is a statistical method that consists on following the path of a series of randomly generated rays through a set of optical elements in the PTC system [27]. First, the energy weight, position and direction of each ray are initialized at the aperture plane by several probability density functions. And then the fate of each ray propagating in the PTC system is determined and recorded by a series of optical events, such as the emissive, reflective, refractive, absorptive and scattering behaviors described by a set of statistical relationships [24,52,56,57]. From these recorded data, the nonuniform distributions of the absorbed solar radiation on the glass cover and/or the absorber tube can be determined and eventually used in a subsequent heat transfer analysis as heat sources [21–28]. With the MCRT method, it is also possible to simulate various optical effects and determine the optical performance of the PTC systems [9,63].

As mentioned above, to develop a general-purpose numerical method or model for improving the design/simulation tools for concentrating solar collectors (CSCs), a new modeling method and homemade unified code with the MCRT method was developed and proposed by the authors in Ref. [56]. It is designed with a new modeling concept of subsystems/layers and some unified solving methods. To help the reader understand, a simplified flowchart is presented in Fig. 2. It can be seen that there are two main loops in the MCRT program. The inner loop is that the photon packet propagates layer by layer. The photon packet is repeatedly moved and traced in a layer once until it escapes from it, or is absorbed by the system, or is killed by a roulette technique to ensure conservation of energy without skewing the distribution of photon deposition when its weight drops below a specified minimum [56,64]. And the outer loop is that this tracing process is repeated until a desired number of photon packets have been propagated. Three coordinate systems are used and can be totally independent from each other. Solar radiation in participating medium and/or non-participating medium can be taken into account simultaneously or dividedly in the simulation. After necessary checking or validating, the solar energy flux density distribution on the absorber wall and the optical performance of the CSC system can be counted. As a preliminary study, the proposed method and code are applied to simulate and analyze the photo-thermal conversion processes in three typical CSCs (i.e., the parabolic trough, the power tower and the dish system). The results show that the proposed method and model are reliable to simulate various types of CSCs. More information about the new designs and the unified MCRT code can be found in Ref. [56] in detail.

In this paper, to present comparative and sensitive analysis for different PTC systems and geometric parameters under different operating conditions, a more detailed optical model for the PTC system is developed, based on the above-mentioned unified MCRT model. Compared to previous PTC optical models [6], it is convenient to model the whole PTC system and add/delete any types of subsystems/layers or surfaces when needed, with the new modeling concept of subsystems/layers and corresponding unified solving methods [56]. And it has the greatest advantage that each subsystem/layer could consist of simpler and fewer surfaces, so that the MCRT calculation of the photon propagation process in the PTC is simplified as just calculating in one simpler layer for one time rather than the whole complex system [56]. From it we can take into account a good number of real circumstances respectively or simultaneously, such as the realistic sun-shape profile, incident angle and surfaces geometry dependent optical properties, wavelength-dependent optical properties, non-orthogonal incidence, tracking errors, imperfect mirror surface, deformation of the parabolic profile, shadow and end effects, light extinction in the media and defo-

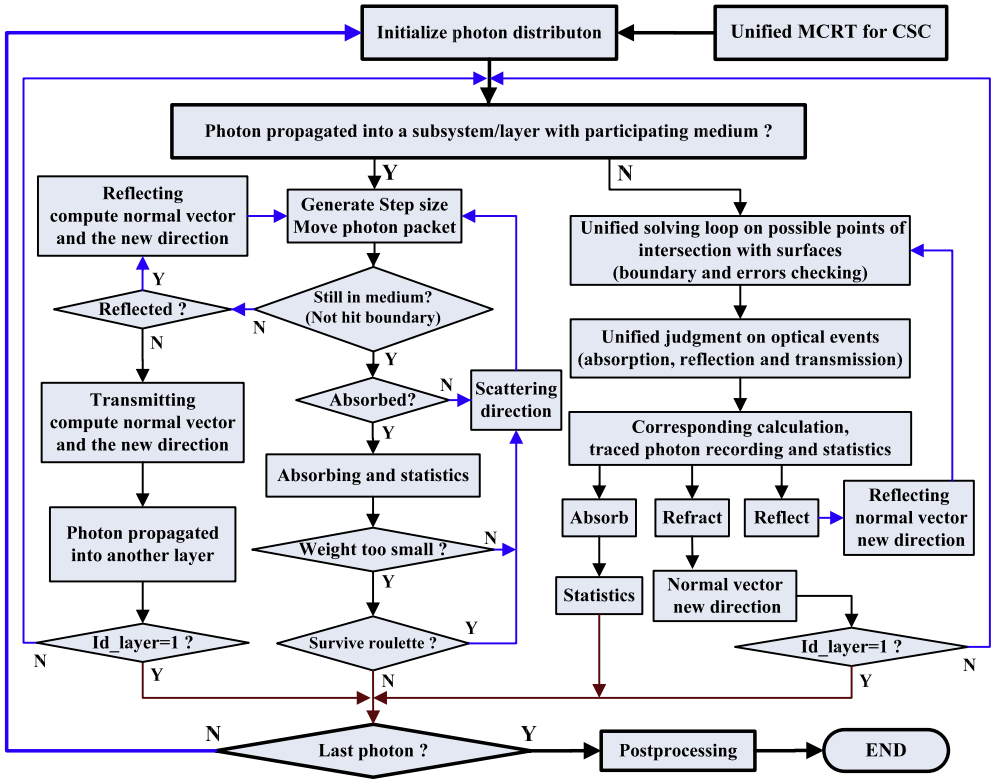

Fig. 2. Flowchart of the unified MCRT code for the solar concentrating and collecting process of the CSCs.

calisation of the receiver. That is, it is capable of estimating the (local or detailed) comprehensive characteristics and optical performance of different practical collectors with various realistic operating conditions. In the model, the incident rays are launched from above the receiver in order to compute correctly the fraction of energy directly absorbed by the receiver, the receiver shadow and the end effects. They are directed at the parabolic reflector surface at a specified non-parallelism incidence angle of 4.65 mrad using a circumsolar ratio (CSR) 5% sunshape angular distribution [9,63]. The rays could also be displaced around the concentrator's axis by a specified value of milliradian if the non-orthogonal incidence or tracking error is simulated. If surface errors are considered, every time the ray hits the reflector a random inclination with Gaussian distribution is added to the theoretical surface normal of the perfect paraboloid at the point of incidence of the ray [6]. For all optical elements, constant values or wavelength dependent optical properties such as the reflectivity, the emissivity or the transmissivity can be used. If some of the optical properties are wavelength-dependent, each ray is split into a number of monochromatic rays with energy weighted according to the ASTM standard AM 1.5 direct spectrums [6,9]. The optical event at each optical element of the PTC system is considered as an all-or-none event and the light is assumed to have no particular polarization [56]. After a simulation, the recorded number of ray intersections in different optical elements of the PTC system allows calculating the absorbed nonuniform solar energy flux density distribution. Based on these statistical data, the characteristics of the concentrated solar flux density distributions (such as the average of the concentrated solar flux density and the nonuniformity of the concentrated solar flux density distributions on the absorber) and the total optical performance of the PTC system can be further obtained, which will be presented detailedly in the following section.

2.3. Parameter definitions

As it is well known, the rays of sunlight are not parallel when the effect of the finite size of the sun is taken into account [12]. Thus a focal shape is always formed around the focal line of the parabolic reflector, caused by the divergence phenomenon of reflected solar beam. If the focal shape width becomes larger than the outer diameter of the absorber (d_a), it may have significant effects on the optical efficiency under some conditions while the absorber cannot collect the entire reflected beam. To study this effect later, here the angular size (or solar radius) $\delta = 16'$ is used to represent the finite size of the sun [45] and thus the width of the focal shape (d_{min}) is theoretically expressed as follows [65]:

$$d_{min} = 2[f + a^2/(16f)]\sin\delta \quad (1)$$

From Eq. (1), some important values of PTC geometric parameters (e.g., a, f, d_a) can be determined from $d_{min} = d_a$ (due to the divergence phenomenon of non-parallel solar beam). They are defined as "critical points" here, which are very useful to analyze the performance characteristics of the PTC system later because the PTC optical performance characteristics change greatly around these points. Details will be presented in the following sections.

The geometric concentration ratio (GC) and the rim angle (φ_m) are specified as follows [12]:

$$GC = a/(\pi d_a) \quad (2)$$

$$\varphi_m = cos^{-1}[(16 - (a/f)^2)/(16 + (a/f)^2)] \quad (3)$$

where a and f are the aperture width and the focal length of the parabolic trough reflector respectively.

The comprehensive characteristics and optical performance studied here includes the characteristics of the maximum and the average of the concentrated solar flux density and the nonuniformity of the concentrated solar flux density distribution on the absorber wall, and the performance of total incident solar radiation, absorbed solar energy and the optical efficiency of the whole PTC system, etc. The average of the concentrated solar flux density on the absorber wall (q_{ave}) is defined as the arithmetic means, as follows:

$$q_{ave} = \frac{\sum_{i=1}^{N_c} q_{SR,i}}{N_c} \quad (4)$$

where N_c is the statistic grid number at the absorber surface, while $q_{SR,i}$ is the local solar flux density of the ith grid.

The nonuniformity of the concentrated solar flux density distributions on the absorber wall (σ_q) is defined as the coefficients of mean deviations, which can be expressed as follows:

$$\sigma_q = \frac{\sum_{i=1}^{N_c} |q_{SR,i} - q_{ave}|}{N_c \cdot q_{ave}} \quad (5)$$

To present and compare the total optical performance of the PTC system under different geometries and real operating conditions, the optical efficiency (η_o) is always specified by the ratio of the statistical absorbed solar radiation ($q_{u,ab}$) to the incident solar radiation on the collector opening ($q_{SR,in}$), as follows:

$$\eta_o = (q_{u,ab}/q_{SR,in}) \times 100\% \quad (6)$$

Note that the efficiency is computed with respect to the solar radiation incident on the collector opening not to the direct normal irradiance (DNI), which already takes into account the cosine effect of the incidence angle for some conditions [6].

3. Code checking and model validation

3.1. Code checking

An independence checking for the total number of photon packets and the grid density of the statistical grid system needs to be performed firstly. At the very start of a MCRT simulation, the total number of photon packets can only be chosen by experience, taking N_{ray} for an example here. As N_{ray} photon packets have been propagated, following the flowchart shown in Fig. 2, the recorded profiles of reflection, transmission and absorption at each surface of the PTC system could be calculated and compared to the known true values. These statistically calculated values mainly depended on the random numbers generated, and the ideal case is to set the total number of photon packets approaches infinity [64]. However, taking the calculation amount and the computing time into account, we should determine a relative large finite number of photon packets (rather than the above-mentioned infinity as required ideally) with an acceptable small error. Some typical checking for the ENEA PTC system was carried out as the same process mentioned in Ref. [56] and a total photon number of 5.0×10^7 is adequate. In addition, the grid density for solar flux statistics is also only chosen by experience at the very start of a MCRT simulation, whereas it can be accurately checked in the same order under the checked total photon number. Since the absorbed solar energy flux density distribution is calculated after the total number of photon packets that have been propagated. Certain it is that much finer the statistical grid system is, more accurate the statistical results are. However, the calculation amount and the computing time are always limiting factors for simulations, so a suitable but minimal grid density for statistics needs to be further determined. This can also be seen in Ref. [56] detailedly.

3.2. Model validation

In order to further confirm the accuracy of the proposed detailed optical model based on the unified MCRT modeling concept for calculating the solar energy flux distribution of the whole PTC system, numerical simulations were carried out with the same collector geometrical configuration, operating conditions, material and optical properties as the ENEA project presented in Ref. [6]. The aperture width of the ENEA PTC system is 6 m, the focal length is 1.8 m, and the outer diameter of the receiver is 70 mm, with a 3 mm thick glass covering of 130 mm in diameter. The reflector also has a small gap of 100 mm, which is also taken into account as mentioned before. The numerical results were compared with that presented in Ref. [6] for some typical real operating conditions such as the realistic sun-shape profile and optical properties and different optical errors. The calculated solar energy flux density distributions on the middle cross-section of the absorber outer surface for an ideal case (i.e., without optical errors), a case of a tracking error (σ_t) of 0.6° and a case of a Gaussian surface error (σ_s) of 0.2° in both directions are presented in Fig. 3 respectively. From the figure, it can be obviously seen that the predicted results agree very well with the results from the reference, which proves that the proposed detailed optical model and the numerical results are reliable.

4. Computational results and discussion

In the following, the comparative analysis for some typical PTC systems available, as the reflectors and the receivers shown in Tables 1 and 2 respectively, will be presented firstly. Later, sensitive studies of the optical characteristics and performance to different PTC geometric parameters and different operating conditions will be carried out. Note that the solar radiation incident on the collector opening is assumed as 1000 W m^{-2} in the simulations, and the ranges of the optical errors studied here are approximately the same with that in Ref. [6]. For each examination, only the corresponding checking parameter varies while all the other parameters remain the same.

4.1. Comparative analysis for PTCs

To make a comparative analysis for some typical PTC systems available, various combinations of seven typical parabolic trough reflectors (i.e., LS-2 Trough [14], LS-3 Trough [10], EuroTrough [10,66], SkyTrough [10], HelioTrough [8], LAT73 Trough [67] and Ultimate Trough [8] listed in Table 1) and four classical evacuated tubular receivers (i.e., LS-2 receiver [10,14], LS-3 receiver [10], Schott PTR70 receiver [68] and Siemens UVAC 2010 receiver [69] listed in Table 2) under the ideal case or optical error conditions are studied preliminarily using the detailed optical model abovementioned. Note that these seven reflectors are labeled as T1 to T7 (see column 1 in Table 1) while these four receivers are labeled

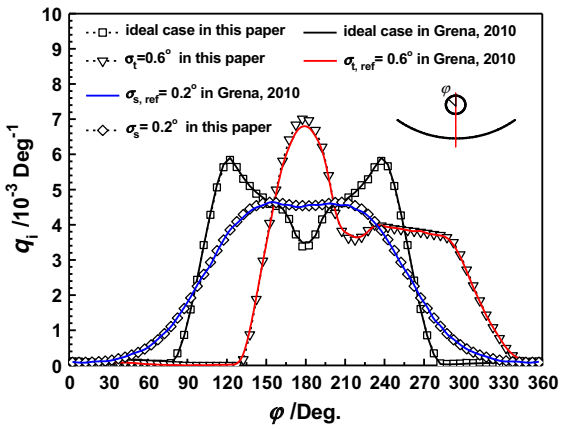

Fig. 3. Model validations for the detailed optical model under some different operating conditions, where q_i and φ are the local solar energy flux density of the ith grid and the angle at the angular direction of the middle absorber cross-section respectively, the solid lines indicate the known data in the reference while the symbolic dotted lines represent the calculated results in this paper.

Table 1
Main characteristics of some typical parabolic trough reflectors.

Cases	Trough names	a (m)	f (m)	φ_m (°)	d_{min} (mm)	ρ_r
T1	LS-2 Trough	5.000	1.490	79.99	23.63	0.940
T2	LS-3 Trough	5.760	1.710	80.20	27.20	0.940
T3	EuroTrough	5.770	1.710	80.30	27.24	0.940
T4	SkyTrough	6.000	1.710	82.51	28.17	0.940
T5	HelioTrough	6.800	1.710	89.66	31.65	0.940
T6	LAT73 Trough	7.300	2.000	84.76	34.12	0.945
T7	Ultimate Trough	7.500	1.880	89.85	34.91	0.944

Table 2
Main characteristics of some typical evacuated tubular receivers.

Cases	Receiver names	d_g (mm)	d_a (mm)	L_r (m)	τ_g	α_a
R1	LS-2 receiver	115	70	3.900	0.950	0.940
R2	LS-3 receiver	115	70	3.900	0.960	0.960
R3	Schott PTR70	125	70	3.926	0.965	0.955
R4	Siemens UVAC 2010	115	70	3.914	0.965	0.960

as R1 to R4 (see column 1 in Table 2) in all subsequent figures. And the reflectors listed in Table 1 are chosen by an increase in aperture width, therefore some systems of similar configurations or aperture widths are not listed or performed separately here, such as the DukeSolar Trough, the SenerTrough, the ENEA Trough and the SKAL-ET. To simplify setting wavelength dependent optical properties that are always difficult to know, wavelength average optical properties are acceptable approximations for simulating relative large-scale troughs [6]. This is also performed in the following simulations by using solar weighted optical properties from references, with the aperture width available varied from 5 m to 7.5 m. It is noted that results of the comparative analysis could be slightly different for different calculating parameters obtained, because there could be variations in geometries or properties from batch to batch provided by the manufacturers or references.

Fig. 4 shows the comparative results for these different PTC systems in the ideal case. From the figure it can be seen that the total incident solar radiation ($q_{SR,in}$) and the statistical absorbed solar energy ($q_{u,ab}$) increase with the increase of the trough number (i.e., T1 to T7 listed in Table 1) as well as the aperture width, while the nonuniformities of solar flux density distributions (σ_q) are of downward trends though the maximal values of solar flux density (q_{max}) become larger and larger. Moreover, the variation trends of σ_q seem to be just the opposite of that of the rim angles (as φ_m listed in Table 1), and the differences of σ_q are inconspicuous between these four receivers. This is generally because a PTC system of a larger rim angle indicates that a larger span of the circumferential angle of the absorber tube can receive higher concentrated solar radiation from the reflector other than the original low solar radiation from the sun directly. It can also be seen that the sixth LAT73 Trough always has the best optical efficiency in these seven reflectors combined with whichever receiver. The fourth Siemens UVAC 2010 receiver always results in the largest absorbed solar energy and the best optical performance, the LS-3 receiver and the Schott PTR70 receiver are the next best configurations, and they are much larger than that of the LS-2 receiver. Furthermore, the values of the total incident solar radiation for these four receivers are not the same even for a specified reflector. It is mainly due to the differences of the active receiver length as listed in Table 2, that is, a larger active length always results in a larger useful total incident solar radiation. However, the variation trends of the absorbed solar energy and the optical efficiency are not in accord with that of the total incident solar radiation. This is because they are also strongly dependent on the optical properties of both the reflectors and the receivers.

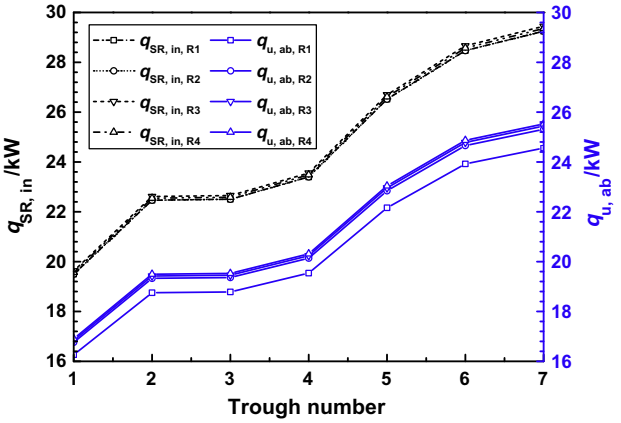

(a) Comparative results for the total incident solar radiation $q_{SR,in}$ and the absorbed solar energy $q_{u,ab}$

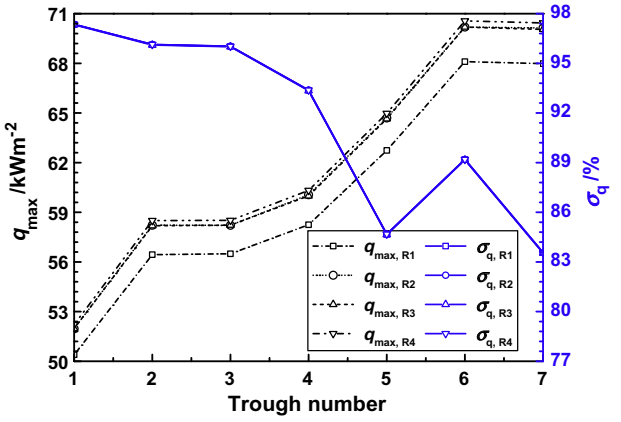

(b) Comparative results for the maximal solar flux density q_{max} and the nonuniformity of the solar flux density distribution σ_q

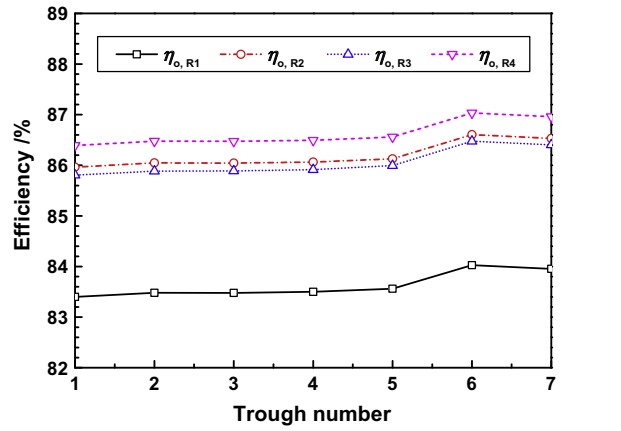

(c) Comparative results for the optical efficiency η_o

Fig. 4. Comparative results for different PTC systems in the ideal case, where the trough number indicates the reflectors listed in Table 1, and R1 to R4 indicates the receivers listed in Table 2.

Fig. 5 shows the comparative results for different PTC systems under the cases of different tracking errors. Fig. 5(a) and (b) shows the optical performance for different reflectors and receivers based on the best Siemens UVAC 2010 receiver and LAT73 Trough mentioned above, respectively. From them following features may be noted. First, η_o and σ_q change slightly under small tracking errors but decrease or increase rapidly after a threshold. And the thresh-

olds are of different values of 6–12 mrad for different reflectors while they are almost constants of about 6 mrad for different receivers with the LAT73 Trough. It may be inferred that different reflectors have different sensitivity to the tracking error that is larger than the corresponding thresholds. Roughly, the larger the aperture width is, the more the reflector is sensitive to the tracking error. Second, the differences between optical efficiencies of different receivers become smaller and smaller with the increase of the tracking error. It could be inferred that the effect of the tracking error becomes the dominant factor when the tracking error continues to increase, as compared to that of the optical properties while all the receivers are of almost the same geometric parameters. Further studies on the effects of geometric parameters of receivers will be carried out separately in the following sections later.

Fig. 6 shows the comparative results for different PTC systems under the cases of different surface errors. Similar variation trends to that of the optical efficiencies under different tracking errors are revealed, but they are more sensitive to the surface errors with very small thresholds of about 2–4 mrad. It can also be seen that σ_q change rapidly with an increase in the surface error at the beginning, but then the variation trend becomes smaller and smaller. The differences between optical efficiencies of different receivers also become smaller with the increase of the surface error, but they are not obvious compared to that with the tracking error increasing. It may be inferred that better optical properties always result in a relative better optical performance, even for an imperfect reflecting surface of larger errors.

A further comparative analysis for different tracking errors and surface errors is presented in Fig. 7, based on the best-combined PTC system of the LAT73 Trough and the Siemens UVAC 2010 receiver (T6R4). Note that all studies in the following sections will also be carried out on this T6R4 PTC system unless otherwise stated. It can be seen from Fig. 7(a) that the PTC system is more sensitive to the surface error than the tracking error. This can also be seen in Fig. 7(b) and (c). With the same interval of 2 mrad, the decreasing trends of optical efficiencies shown in Fig. 7(b) under different surface errors are obviously larger than that shown in Fig. 7(c) under different tracking errors. In addition, there is an interesting thing can be found in Fig. 7(b) that a larger surface error corresponds to a higher optical efficiency for a specified tracking error larger than 14 mrad, where relative variation trends of different surface errors are totally inversed. However, it may not be a desirable way to obtain a higher optical performance under such a large tracking error for real uses. From Fig. 7(c) it can also be seen that the differences between curves of different tracking errors become smaller and smaller when the surface error becomes relative large. This may be because the much larger surface error has become the leading factor in the optical efficiency, compared to the tracking error. It can therefore be concluded that extra care should be taken in constructing the parabolic surface.

4.2. Effects of varying reflector parameters

As we know, an ideal parabolic trough reflector can be mainly determined by a focal length f and an aperture width a.

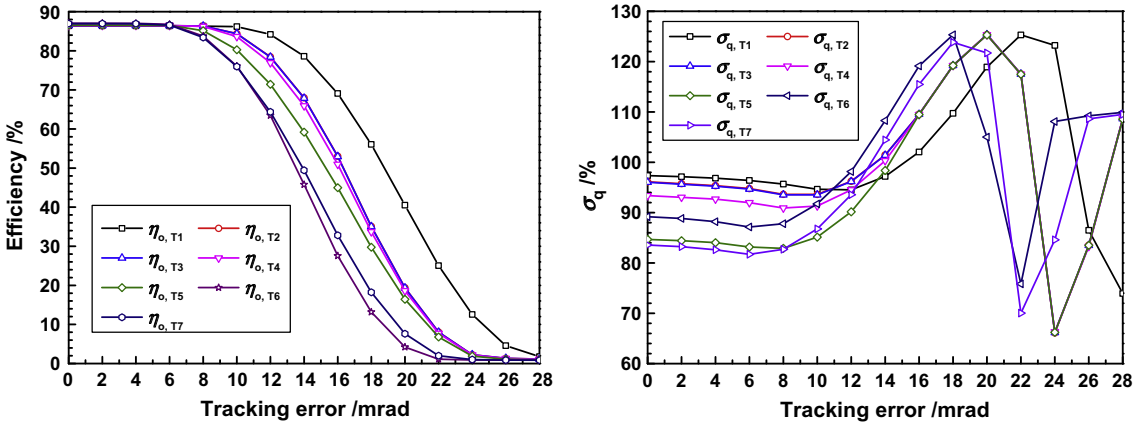

(a) Optical characteristics and performance for different reflectors with the UVAC 2010 receiver (R4)

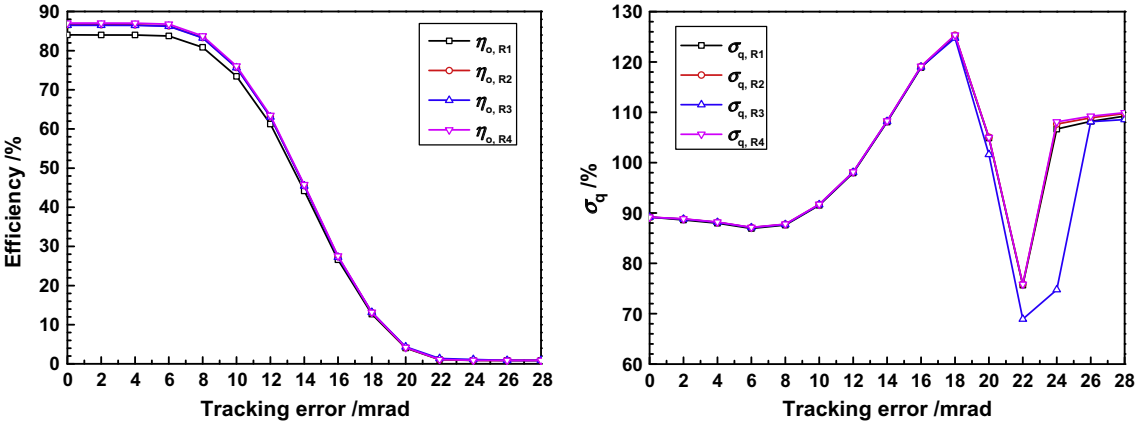

(b) Optical characteristics and performance for different receivers with the LAT73 Trough (T6)

Fig. 5. Comparative results for different PTC systems under the cases of different tracking errors, where η_o and σ_q are the optical efficiency and the nonuniformity of the solar flux density distribution respectively, T1 to T7 indicates the reflectors listed in Table 1, and R1 to R4 indicates the receivers listed in Table 2.

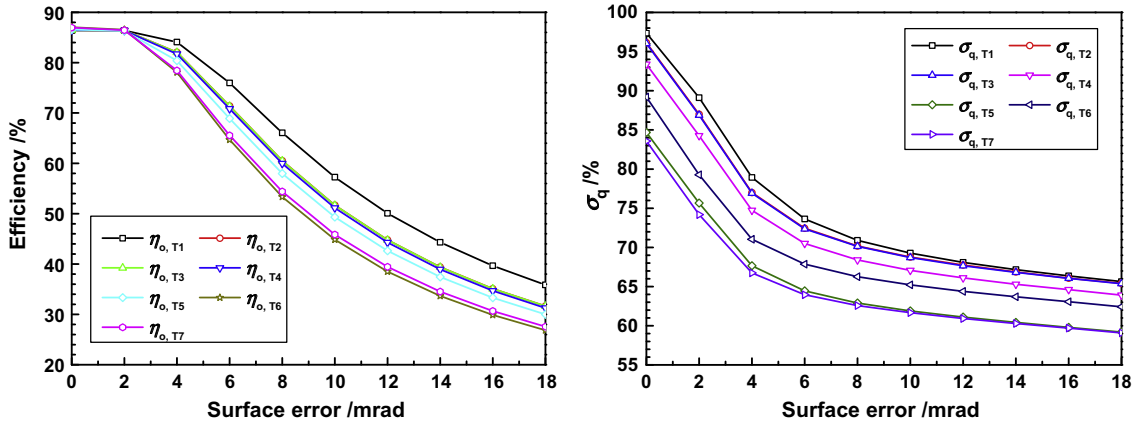

(a) Optical characteristics and performance for different reflectors with the UVAC 2010 receiver (R4)

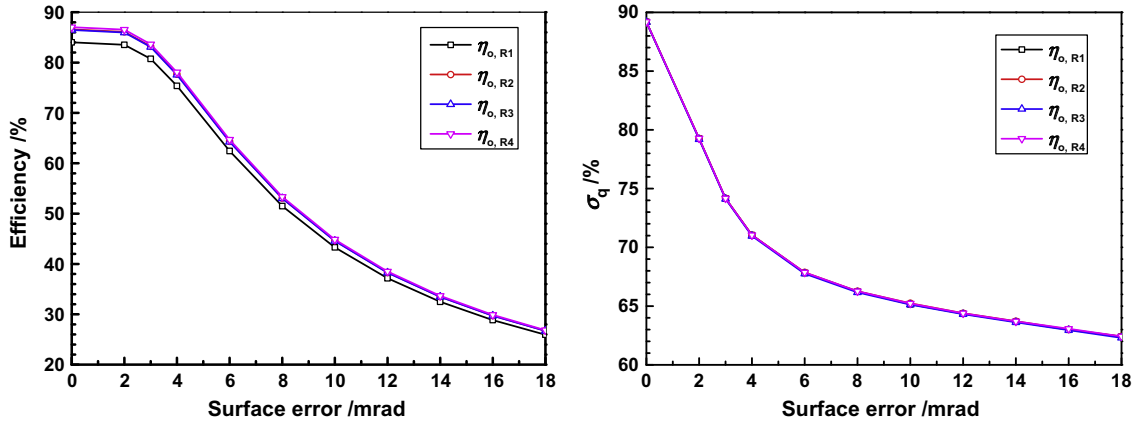

(b) Optical characteristics and performance for different receivers with the LAT73 Trough (T6)

Fig. 6. Comparative results for different PTC systems under the cases of different surface errors, where η_o and σ_q are the optical efficiency and the nonuniformity of the solar flux density distribution respectively, T1 to T7 indicates the reflectors listed in Table 1, and R1 to R4 indicates the receivers listed in Table 2.

In the following, the results of comparative and sensitive analysis on the T6R4 PTC system of different a and f under different operating conditions will be presented, respectively.

4.2.1. Effects of varying the aperture width

Fig. 8(a) and (b) shows the effects of varying the aperture width (a) on the optical characteristics and performance of the PTC systems in the ideal case. From them following features may be noted. First, q_{max} and q_{ave} increase with the increase of a, while σ_q decreases rapidly with a increasing firstly. Then all variation trends change slightly with further increase in a when it is larger than 13.3 m. Second, $q_{SR,in}$ and $q_{u,ab}$ always increase with a increasing but they are of different variation trends. The absolute difference between them becomes larger and larger. $q_{u,ab}$ first increases rapidly as a increased, but eventually the increasing trend decreases, while $q_{SR,in}$ is always proportional to a. Third, η_o first increases with the increase of a, reaching an ideal maximum of 87.20% at $a \approx 13.3$ m, and then it decreases greatly with a further increase in a.

The reasons can be inferred from the theoretical analysis results shown in Fig. 8(c) clearly. It can be seen that the value of GC is always proportional to a while d_a keeps the constant of 70 mm. The values of φ_m and d_{min} increase with an increase in a though they are of different variation trends. As mentioned before, the variation trend of σ_q is just the opposite of the ratio of φ_m to the whole absorber circumferential angle 2π. Since a larger rim angle generally indicates a larger span of the absorber circumferential angle can receive higher concentrated solar radiation from the reflector other than the original low solar radiation from the sun directly. For the optical performance, the absorber can collect the entire reflected beam from the reflector for $d_{min} \leqslant d_a$ when a increases from a relative small value to about 13.3 m (i.e., the critical point derived from $d_{min} = d_a$). Therefore, $q_{u,ab}$ and η_o increases with the increase of a firstly. However, the increasing trend of $q_{u,ab}$ decreases when a is larger than 13.3 m for $d_{min} > d_a$, due to the fact that the absorber starts losing the reflected beam from this critical point, and thus η_o drops significantly. From the discussion it is also revealed that the numerical results can be well explained by the theoretical analysis results, also proving that the numerical model used in the present study is reliable.

Fig. 8(d) shows the results of sensitivity analysis of the optical performance to different a under different optical errors. It can be obviously seen that the introduced PTC systems of different a values have different sensitivity to the optical errors such as the tracking error and the surface error. The larger the aperture width is, the more the PTC system is sensitive to the optical errors. Moreover, the levels of sensitivity to different optical errors are very different. To obtain a relative higher optical efficiency (of an intercept factor exceeding 98% [67]), the tracking error and the surface error are suggested to be smaller than about 6 mrad and 2 mrad respectively, for most of the available PTC systems with the aperture width varies from 5.0 m to 7.5 m. Generally, a larger aperture width always representatives a larger incident solar radiation, while a larger absorber diameter can be chosen to collect the entire reflected beam from the relative larger reflector. Thus, the next generation of the LAT PTC system is declared to be of 10 m in aper-

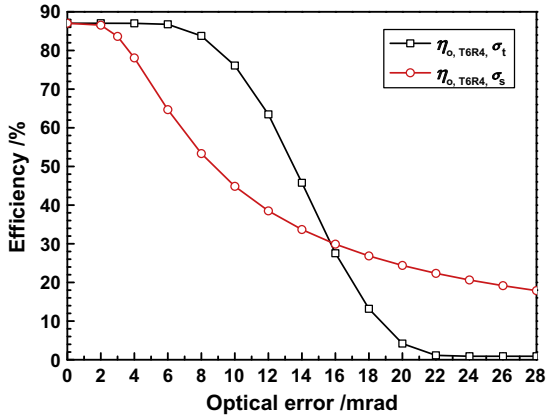

(a) Comparative analysis for different optical errors

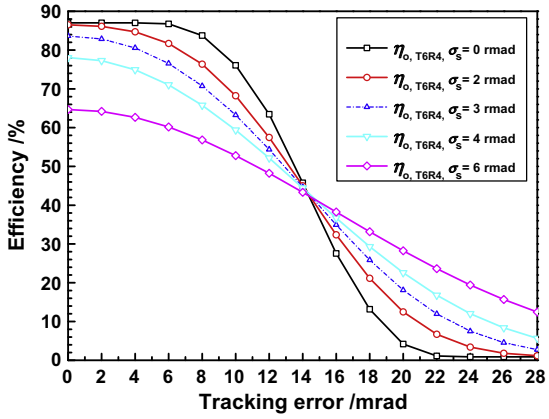

(b) Sensitivity to surface errors σ_s under different tracking errors σ_t

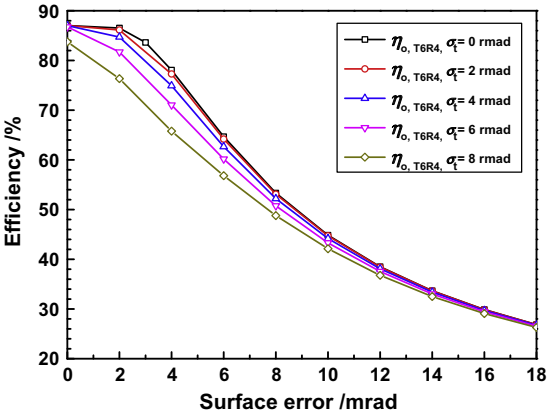

(c) Sensitivity to tracking errors σ_t under different surface errors σ_s

Fig. 7. Comparative analysis and sensitivity analysis for different tracking errors σ_t and surface errors σ_s.

ture width and 90 mm in absorber diameter. However, form the figure it can be seen that more strict operating conditions or great efforts on accuracy of manufacture are required to maintain a higher optical performance for a larger PTC, since a larger reflector is more sensitive to these factors. Moreover, a larger receiver dimension may result in a larger heat loss, thus the thermal performance also needs to be further investigated as well as the optical performance. That is, studies on the total efficiency of the whole photothermal process of the PTC system needs to be further carried out later to obtain an optimized configuration, by combining the absorbed nonuniform solar flux density distributions calculated by this proposed model into a subsequent heat transfer analysis as heat sources [21–28].

4.2.2. Effects of varying the focal length

Fig. 9(a) and (b) shows the effects of varying the focal length (f) on the optical characteristics and performance of the PTC systems in the ideal case. From them it can be seen that q_{max} and σ_q decrease with an increase in f firstly, and then they increase with a further increase in f, while q_{ave} and $q_{SR,in}$ are almost constants with the unchanged aperture width of 7.3 m. $q_{u,ab}$ and η_o are of the same variation trends with f increasing which is different from that of different a above-mentioned. That is, they first increase with the decrease of f, reaching the ideal maximums of 24.94 kW and 87.28% respectively at $f \approx 0.47$ m, and then they decrease greatly with a further decrease in f.

This can also be inferred from the theoretical analysis results shown in Fig. 9(c) clearly. It can be seen that GC is always unchanged with the constant aperture width. The variation trend of σ_q is also the opposite of the ratio of φ_m to the whole absorber circumferential angle when the focal length is larger than 0.47 m, but it becomes inversed while the focal length becomes smaller than 0.47 m. d_{min} first decreases and then increases with the increase of f.

Therefore, there are two values of f equal to about 0.47 m and 7.05 m for $d_{min} = d_a$ (i.e., critical points), which can also be inferred from Eq. (1). The relative larger focal length of 7.05 m could not be appropriate for a PTC system but for a large-scale linear Fresnel collector system with a stationary receiver far away from the reflector or the ground, which is not discussed here. The smaller one of 0.47 m theoretically corresponds to the best optical efficiency under the condition studied in this paper. The reasons can be presented as follows. When f decreases from a relative large value to about 0.47 m, the absorber can collect the entire reflected beam from the reflector for $d_{min} \leqslant d_a$, thus $q_{u,ab}$ and η_o increases with the decrease of f firstly. Whereas f becomes smaller than 0.47 m, both $q_{u,ab}$ and η_o drop significantly due to the effects of the divergence of reflected beam for $d_{min} > d_a$ shown in Fig. 9(c). From these results of the effects of different a and f, it could be inferred that the characteristics and performance of a PTC system are always affected by some critical points determined from the divergence phenomenon of the non-parallel solar beam. Moreover, this may be very useful sometimes to provide some reference for designing a better PTC system.

Fig. 9(d) shows the results of sensitivity analysis of the optical performance to different f under different optical errors. It can be obviously seen that the introduced PTC systems of different f values also have different levels of sensitivity to the tracking error and the surface error. The PTC systems are still more sensitive to the surface error than the tracking error. Moreover, there is a range of the focal length varies from 1.0 m to 2.0 m with an relative higher optical efficiency (of an intercept factor exceeding 98% [67]) while the tracking error and the surface error is within about 6 mrad and 2 mrad respectively. Outside this range, the optical efficiency drops rapidly even for a small tracking error or surface error. On the other hand, the differences of the optical efficiency between every two optical error cases become larger and larger when the focal length becomes much larger than the upper bound ($\gg$2.0 m). It may mean that a PTC system of a larger focal length is more sensitive to a larger optical error.

4.3. Effects of varying receiver parameters

In the following, the results of comparative and sensitive analysis on different geometric parameters of the receiver, such as the longitudinal active receiver length (L_r), the glass cover diameter

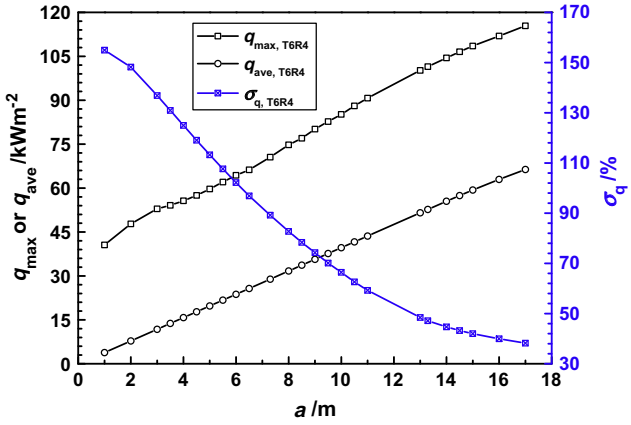

(a) Variations of the maximal solar flux density q_{max}, the average solar energy flux density q_{ave} and the nonuniformity of the solar flux density distribution σ_q with the aperture width a

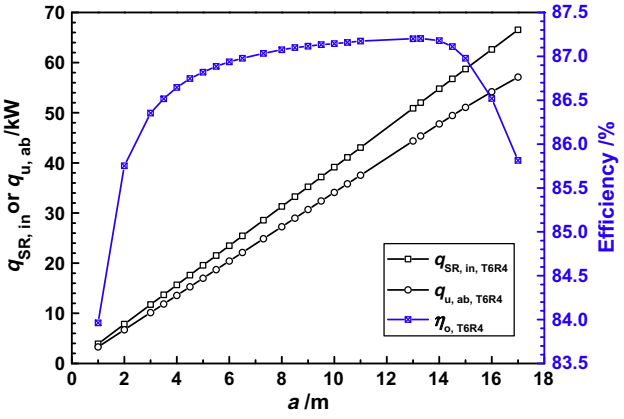

(b) Variations of the total incident solar radiation $q_{SR,in}$, the absorbed solar energy $q_{u,ab}$ and the optical efficiency η_o with the aperture width a

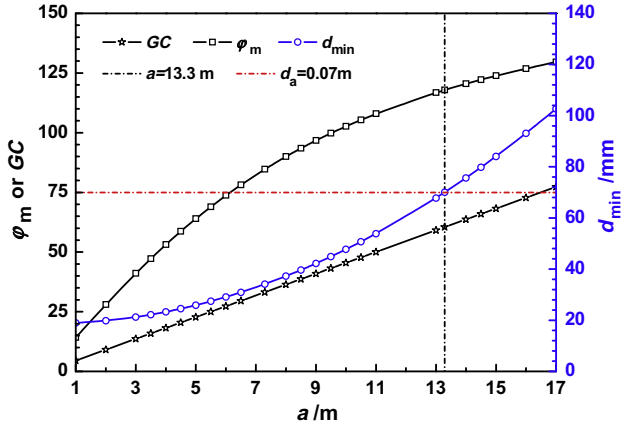

(c) Variations of the geometric concentration ratio GC, the rim angle φ_m and the width of the focal shape d_{min} with the aperture width a

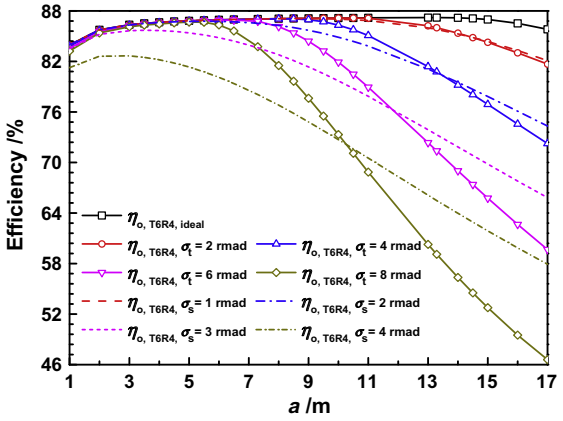

(d) The optical efficiency η_o as a function of the aperture width a under different optical errors

Fig. 8. Effects of varying the aperture width a on comprehensive characteristics and optical performance of the PTC system.

(d_g) and the absorber diameter (d_a), will be presented under some different operating conditions in order.

4.3.1. Effects of varying the active receiver length

As we know, most of the present receivers are of 4.06 m in total length, but they are of different values of the active length as seen in Table 2. The active area-to-length ratio of the active length to the total length could stand for the level of receiver manufactures in some ways. Because the larger the active receiver length is, the shorter the metal bellows and the glass-to-metal joints are. As a result, the requirement of maintaining the necessary vacuum-tight enclosure and accommodating for the thermal expansion difference between the glass cover and the steel absorber becomes more and more strict.

We examined the effects of varying the active receiver length (L_r) on the optical characteristics and performance of the PTC systems in the ideal case. In the examination, L_r varies from 3.90 to 3.96 m and thus the corresponding active area-to-length ratio varies from 96% to 97.5%. It is revealed that both σ_q and η_o change slightly with the increase of L_r, though both $q_{SR,in}$ and $q_{u,ab}$ increase by about 1.5% (i.e., they changed from 28.47 kW to 28.91 kW and from 24.78 kW to 25.16 kW respectively). There is a very small increasing trend in η_o as L_r increased. It may due to the decrease of the ratio of the photon packets lost from the receiver ends to the total incident photon packets, with a relative larger active receiver length. In addition, the PTC systems of different active receiver lengths studied here have little sensitivity to the optical errors.

4.3.2. Effects of varying the glass cover diameter

Fig. 10(a) shows the effects of varying the glass cover diameter (d_g) on the optical characteristics and performance of the PTC systems in the ideal case. It can be noted from this figure that both σ_q and η_o decrease with the increase of d_g, but the variation trends are very small. They change less than 0.4% as the glass cover diameter varied from 80 mm to 130 mm while the absorber keeps a constant of 70 mm in diameter. From a detailed analysis it can be inferred that the glass cover mainly influence the trajectories of the photon packets propagating in the annular space between the glass cover and the absorber tube, and a larger glass cover diameter means a larger annular space for the photon packets escaping from it. To check this, a larger absorber diameter of 90 mm which will be used for the next generation of the LAT PTC system mentioned before is further studied. It can be obviously seen that η_o is larger than that of the absorber of 70 mm under a specified value of d_g, but σ_q also becomes larger. More information about the effects of the absorber diameter on the optical characteristics and performance of the PTC systems will be further presented in the following section. Fig. 10(b) shows the results of sensitivity analysis of the optical

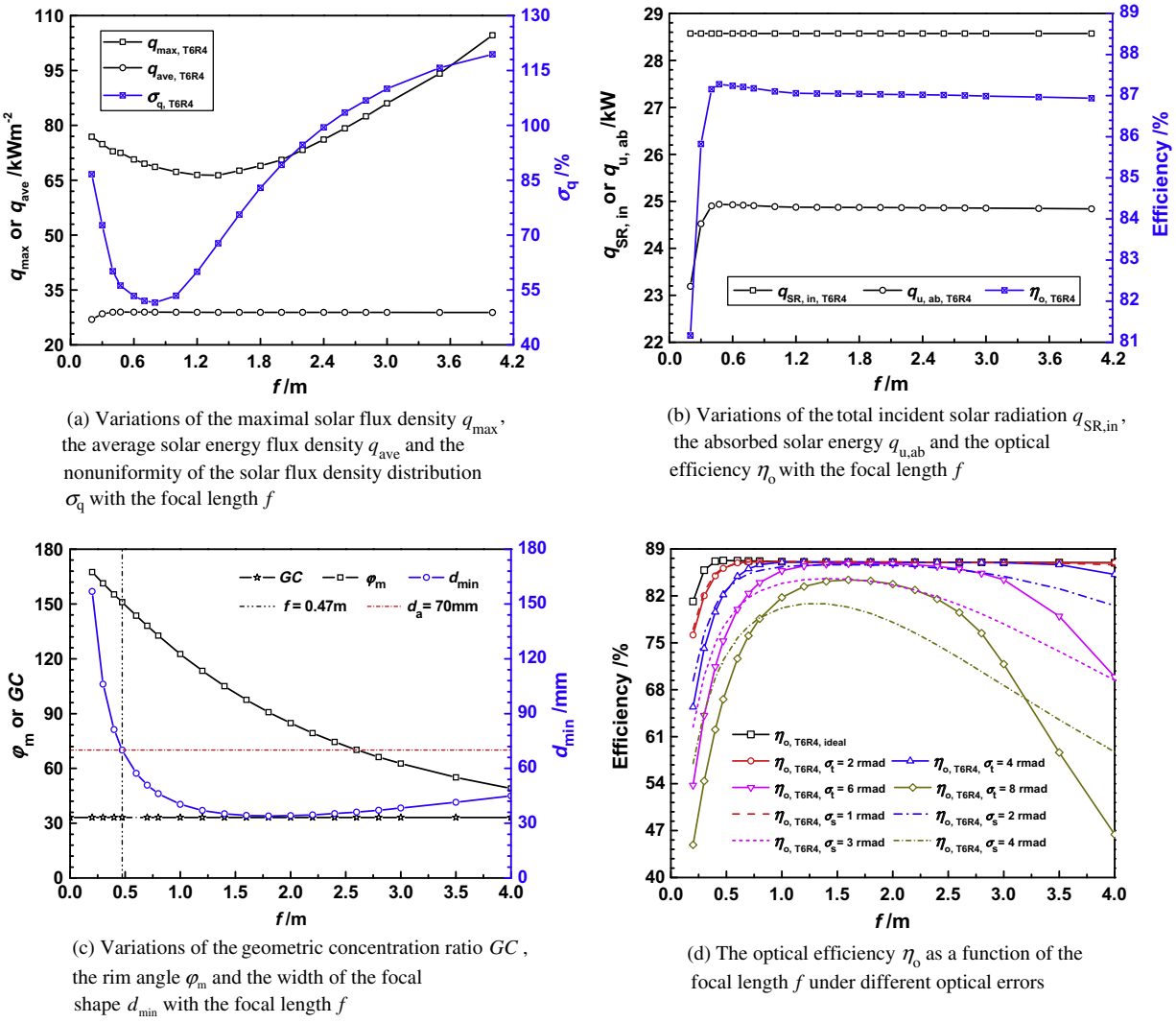

(a) Variations of the maximal solar flux density q_{max}, the average solar energy flux density q_{ave} and the nonuniformity of the solar flux density distribution σ_q with the focal length f

(b) Variations of the total incident solar radiation $q_{SR,in}$, the absorbed solar energy $q_{u,ab}$ and the optical efficiency η_o with the focal length f

(c) Variations of the geometric concentration ratio GC, the rim angle φ_m and the width of the focal shape d_{min} with the focal length f

(d) The optical efficiency η_o as a function of the focal length f under different optical errors

Fig. 9. Effects of varying the focal length f on comprehensive characteristics and optical performance of the PTC system.

performance to different d_g under different optical errors. It is clear from the figure that the PTC systems of different glass cover diameters have little sensitivity to neither the tracking error nor the surface error. Overall, an optimized glass cover diameter could be obtained by taking into account the optical efficiency, the heat loss around the glass tube, the absorber size, and the manufacture of glass-to-metal joints, etc.

4.3.3. Effects of varying the absorber diameter

Fig. 11(a) shows the effects of varying the absorber diameter (d_a) on the optical characteristics and performance of the PTC systems in the ideal case. From the figure it can be seen that both σ_q and η_o increase with the increase of d_a, and the variation trends are much larger than that of d_g, especially for the former nonuniformities of solar flux density distributions. Though φ_m is not changed, the ratio of the angle receiving higher concentrated solar radiation from the reflector to the whole absorber circumferential angle becomes smaller as d_a increased, thus σ_q increase accordingly. However, the larger the absorber is, the smaller the annular space is, and thus the less the photon packets propagating in the annular space can escape from it. As a result, η_o increase about 1.1% as the absorber diameter varies from 30 mm to 100 mm. In addition, there is a sudden drop of η_o when d_a is smaller than about 34.12 mm. This is due to the fact that the absorber diameter becomes smaller than the focal shape width (as d_{min} listed in Table 1), and thus the absorber also starts losing reflected beam from this critical point that is also derived from $d_{min} = d_a$.

Fig. 11(b) shows the results of sensitivity analysis of the optical performance to different d_a under different optical errors. It can be obviously seen that the introduced receivers of different d_a have different sensitivity to the tracking error or the surface error. The smaller the absorber diameter is, the more sensitive the whole PTC system to the optical errors is. To obtain an a relative higher optical efficiency (of an intercept factor exceeding 98% [67]) for most of the available receivers of 70 mm in diameter, the tracking error and the surface error are suggested to be smaller than about 6 mrad and 2 mrad, respectively. It is certain that a larger optical error is acceptable for a larger absorber. Moreover, this accuracy requirement is well in accord with that of the reflectors of different aperture widths or focal lengths mentioned before, which may also mean that the optical accuracy requirements from different geometric parameters of the whole PTC system are always consistent.

5. Conclusions

This study presented numerical results of comparative analysis for some typical PTC systems available and sensitive studies on effects of main geometric parameters on the comprehensive charac-

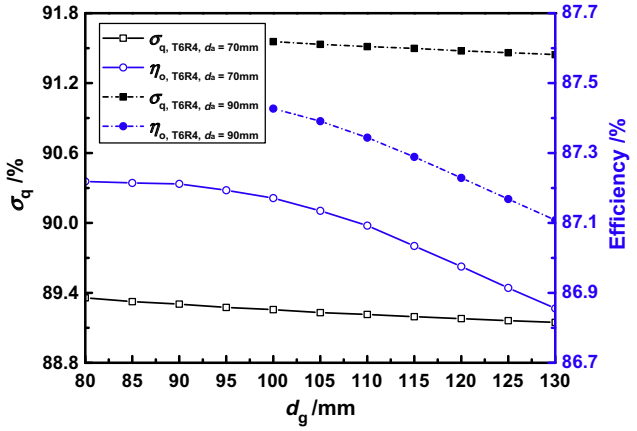

(a) Variations of the nonuniformity of the solar flux density distribution σ_q and the optical efficiency η_o with the glass cover diameter d_g in the ideal case

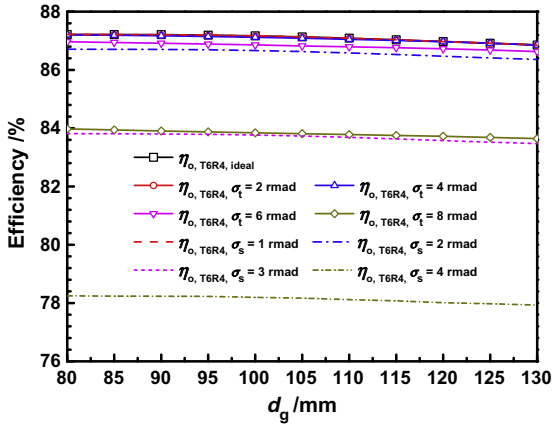

(b) The optical efficiency η_o as a function of the glass cover diameter d_g under different optical errors

Fig. 10. Effects of varying the glass cover diameter d_g on comprehensive characteristics and optical performance of the PTC system.

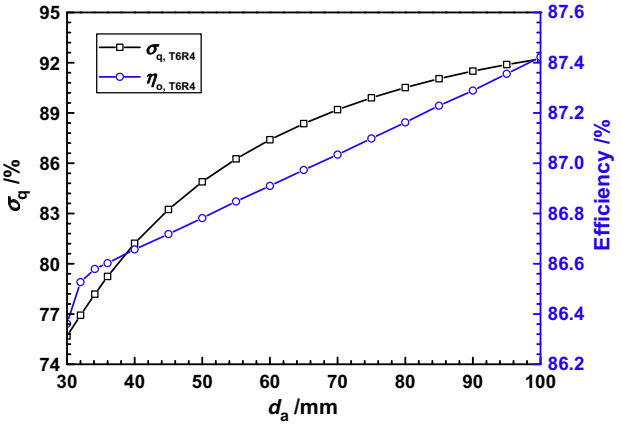

(a) Variations of the nonuniformity of the solar flux density distribution σ_q and the optical efficiency η_o with the absorber diameter d_a in the ideal case

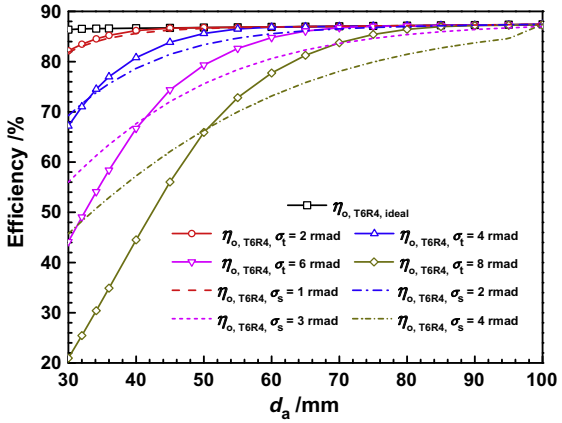

(b) The optical efficiency η_o as a function of the absorber diameter d_a under different optical errors

Fig. 11. Effects of varying the absorber diameter d_a on comprehensive characteristics and optical performance of the PTC system.

teristics/optical performance of the PTC systems under different operating conditions. This work was carried out by a more detailed optical model developed from the previously proposed unified MCRT model after necessary model validations, expecting to optimize the PTC system of better comprehensive characteristics and optical performance or to evaluate the accuracy required for future constructions. The following conclusions can be made.

(1) It is revealed that the numerical results agree well with the reference data, proving that the optical model and the numerical method used in the present study are feasible and reliable. The numerical results can also be well explained by the theoretical analysis results. And it is revealed that the comprehensive characteristics and optical performance of the PTC systems are very different from some critical points determined by the divergence phenomenon of the non-parallel solar beam. From these critical points, the optional geometric parameters can be optimized to obtain relative better PTC performance.

(2) From the comparative analysis, it is found that the LAT73 Trough has the best optical efficiency while the Siemens UVAC 2010 receiver results in the largest absorbed solar energy and the best optical performance under the condition studied. The total incident solar radiation and the statistical absorbed solar energy increase with the increase of the aperture width and the active receiver length. The nonuniformity of the solar flux density distribution is strongly associated with the ratio of the angles receiving higher concentrated solar radiation from the reflector to the whole absorber circumferential angle. There are different threshold values of about 6–12 mrad in the tracking error and about 2–4 mrad in the surface error to remain a relative higher optical efficiency. Different reflectors also have different sensitivity to the optical errors larger than these corresponding thresholds, and the PTC systems are more sensitive to the surface error than the tracking error. It can therefore be concluded that extra care should be taken in constructing the parabolic surface.

(3) From the analysis on the T6R4 PTC system of different aperture widths under some operating conditions, an ideal optimized aperture width of 13.3 m, with a maximum optical efficiency of 87.20%, can be determined by taking into account the effects of the divergence of the non-parallel solar beam. The PTC systems of different aperture widths have different levels of sensitivity to different optical errors. The larger the aperture width is, the more sensitive the PTC system to the optical errors is. For most of the available PTC systems with the aperture width varies from 5.0 m to 7.5 m, the tracking error and the surface error are suggested to be smaller than about 6 mrad and 2 mrad respectively.

(4) From the analysis on the T6R4 PTC system of different focal lengths under some operating conditions, it could also be inferred that the characteristics and performance of a PTC system are affected by two critical points determined from the effects of the divergence of the non-parallel solar beam. This may be very useful sometimes to provide some reference data for designing a better PTC system. Therefore, an ideal optimized focal length of 0.47 m can be determined accordingly, with a maximum optical efficiency of 87.28%. The PTC systems of different focal lengths also have different levels of sensitivity to different optical errors and they are still more sensitive to the surface error than the tracking error. Moreover, there is a range of the focal length varies from 1.0 m to 2.0 m with relative higher optical efficiencies while the tracking error and the surface error is within about 6 mrad and 2 mrad respectively. Outside this range, the optical efficiency drops rapidly even for a small tracking error or surface error.

(5) Under the conditions studied, the PTC systems of different active receiver lengths or different glass cover diameters have little effects on the optical performance and little sensitivity to the optical errors. However, the PTC systems of different absorber diameters have relative larger effects than that of them. They also have different sensitivity to the tracking error and the surface error. The smaller the absorber diameter is, the more sensitive the whole PTC system to the optical errors is. To obtain a relative higher optical efficiency for most of the available receivers of 70 mm in diameter, the tracking error and the surface error are suggested to be smaller than about 6 mrad and 2 mrad, respectively. It is certain that a larger optical error can be acceptable for a larger absorber.

(6) Moreover, the accuracy requirement of the receivers for optical errors is well in accord with that of the reflectors of different aperture widths or focal lengths, meaning that the optical accuracy requirements from different geometric parameters of the whole PTC system are always consistent. However, there may be some contradictory trends in the optical efficiency and the thermal efficiency for optimizing some geometric parameters, such as the glass cover diameter mentioned before. To obtain a better PTC system of a higher total efficiency (i.e., solar to net heat efficiency), investigations on the whole photo-thermal process of the PTC system under real operating conditions over a year need to be further performed and are currently performed, by combining the absorbed nonuniform solar radiation distributions calculated by this model into a subsequent heat transfer analysis as heat sources.

Acknowledgements

The study is supported by the National Natural Science Foundation of China (No. 51306149) and the Research Project of Chinese Ministry of Education (Nos. 20120201130006, 113055A).

References

[1] Tian Y, Zhao CY. A review of solar collectors and thermal energy storage in solar thermal applications. Appl Energy 2013;104:538–53.
[2] Geyer M. International market introduction of concentrated solar power-policies and benefits. In: Proceedings of ISES solar world congress 2007: solar energy and human settlement, vol. 1, Beijing, China, September 18–21, 2007. p. 75–82.
[3] Porta FL. Technical and economical analysis of future perspectives of solar thermal power plants. Report of IER; 2005.
[4] Kalogirou SA. Solar thermal collectors and applications. Prog Energy Combust Sci 2004;30(3):231–95.
[5] Bekhit A, Khalil A, Kaseb S, Othman H. HelioTrough thermal performance compared to EuroTrough. In: 2012 First international conference on renewable energies and vehicular technology, Hammamet, Tunisia, March 26–28, 2012. p. 344–47.
[6] Grena R. Optical simulation of a parabolic solar trough collector. Int J Sustain Energy 2010;29(1):19–36.
[7] Price H, Lüpfert E, Kearney D, Zarza E, Cohen G, Gee R, et al. Advances in parabolic trough solar power technology. J Sol Energy Eng 2002;124:109–25.
[8] Schiel W. Collector development for solar parabolic trough power plants. Bautechnik 2012;89(3):182–91.
[9] Wirz M, Roesle M, Steinfeld A. Three-dimensional optical and thermal numerical model of solar tubular receivers in parabolic trough concentrators. J Sol Energy Eng 2012;134:041012-1–2-9.
[10] Fernández-García A, Zarza E, Valenzuela L, Pérez M. Parabolic-trough solar collectors and their applications. Renew Sustain Energy Rev 2010;14:1695–721.
[11] Yang B, Zhao J, Yao WB, Zhu Q, Qu H. Feasibility and potential of parabolic trough solar thermal power plants in Tibet of China. In: Power and energy engineering conference (APPEEC) 2010 Asia-Pacific, Chengdu, China, March 28–31, 2010. p. 1–4.
[12] He YL, Xiao J, Cheng ZD, Tao YB. A MCRT and FVM coupled simulation method for energy conversion process in parabolic trough solar collector. Renew Energy 2011;36:976–85.
[13] He YL, Cheng ZD, Cui FQ, Li ZY, Li D. Numerical investigations on a pressurized volumetric receiver: solar concentrating and collecting modelling. Renew Energy 2012;44:368–79.
[14] Dudley V, Kolb G, Sloan M, Kearney D. SEGS LS2 solar collector – test results. Report of Sandia National Laboratories, SANDIA 94-1884, USA; 1994.
[15] Odeh SD, Morrison GL, Behnia M. Modelling of parabolic trough direct steam generation solar collectors. Sol Energy 1998;62(6):395–406.
[16] Forristall R. Heat transfer analysis and modeling of a parabolic trough solar receiver implemented in engineering equation solver. Technical report, NREL/TP-550-34169; 2003.
[17] Eskin N. Transient performance analysis of cylindrical parabolic concentrating collectors and comparison with experimental results. Energy Convers Manage 1999;40:175–91.
[18] Eck M, Steinmann WD. Modelling and design of direct solar steam generating collector fields. J Sol Energy Eng 2005;127:371–80.
[19] Naeeni N, Yaghoubi M. Analysis of wind flow around a parabolic collector (1) fluid flow. Renew Energy 2007;32:1898–916.
[20] Naeeni N, Yaghoubi M. Analysis of wind flow around a parabolic collector (2) heat transfer from receiver tube. Renew Energy 2007;32:1259–72.
[21] Cheng ZD, He YL, Xiao J, Tao YB, Xu RJ. Numerical study of heat transfer characteristics in the solar receiver tube combined with MCRT method. In: 2009 Inaugural US-EU-China thermophysics conference – renewable energy, Beijing, China, May 28–30, 2009.
[22] Cheng ZD, He YL, Xiao J, Tao YB, Xu RJ. Three-dimensional numerical study of heat transfer characteristics in the receiver tube of parabolic trough solar collector. Int Commun Heat Mass 2010;37(7):782–7.
[23] Eck M, Feldhoff JF, Uhlig R. Thermal modelling and simulation of parabolic trough receiver tubes. In: Proceedings of the ASME 4th international conference on energy sustainability 2010, Phoenix, Arizona, USA, May 17–22; 2010, p. 1–8.
[24] Wang FQ, Shuai Y, Yuan Y, Yang G, Tan HP. Thermal stress analysis of eccentric tube receiver using concentrated solar radiation. Sol Energy 2010;84:1809–15.
[25] Cheng ZD, He YL, Cui FQ, Xu RJ, Tao YB. Numerical simulation of a parabolic trough solar collector with nonuniform solar flux conditions by coupling FVM and MCRT method. Sol Energy 2012;86(6):1770–84.
[26] Cheng ZD, He YL, Cui FQ. Numerical study of heat transfer enhancement by unilateral longitudinal vortex generators inside parabolic trough solar receivers. Int J Heat Mass Transfer 2012;55:5631–41.
[27] Silva R, Pérez M, Fernández-Garcia A. Modeling and co-simulation of a parabolic trough solar plant for industrial process heat. Appl Energy 2013;106:287–300.
[28] Wang P, Liu DY, Xu C. Numerical study of heat transfer enhancement in the receiver tube of direct steam generation with parabolic trough by inserting metal foams. Appl Energy 2013;102:449–60.
[29] Kalogirou SA. A detailed thermal model of a parabolic trough collector receiver. Energy 2012;48(1):298–306.
[30] Manzolini G, Giostri A, Saccilotto C, Silva P, Macchi E. Development of an innovative code for the design of thermodynamic solar power plants Part A: Code description and test case. Renew Energy 2011;36:1993–2003.
[31] Padilla RV, Demirkaya G, Goswami DY, Stefanakos E, Rahman MM. Heat transfer analysis of parabolic trough solar receiver. Appl Energy 2011;88:5097–110.
[32] Wang J, Huang XY, Gong GJ, Hao ML, Yin FF. A systematic study of the residual gas effect on vacuum solar receiver. Energy Convers Manage 2011;52:2367–72.
[33] Daniel P, Joshi Y, Das AK. Numerical investigation of parabolic trough receiver performance with outer vacuum shell. Sol Energy 2011;85:1910–4.
[34] Burkholder F, Brandemuehl M, Price H, Netter J, Kutscher C, Wolfrum E. Parabolic trough receiver thermal testing. In: Proceedings of ES2007 energy

sustainability 2007, Long Beach, California, USA, June 27–30, 2007. p. ES2007-36129.
[35] Lüpfert E, Riffelmann K-J, Price H, Burkholder F, Moss T. Experimental analysis of overall thermal properties of parabolic trough receivers. J Sol Energy Eng 2008;130:021007-1–7-5.
[36] Burkholder F, Kutscher C. Heat-loss testing of Solel's UVAC3 parabolic trough receiver. Technical report NREL/TP-550-42394, NREL, USA; 2008.
[37] Burkholder F, Kutscher C. Heat loss testing of Schott's 2008 PTR70 parabolic trough receiver. Technical report NREL/TP-550-45633, NREL, USA; 2009.
[38] Petrasch J. A free and open source Monte Carlo ray tracing program for concentrating solar energy research. In: Proceedings of ASME 2010 4th international conference on energy sustainability ES2010, Phoenix, Arizona, USA, May 17–22, 2010. p. ES2010-90206.
[39] Burkhard DG, Shealy DL, Sexl RU. Specular reflection of heat radiation from an arbitrary reflection of heat radiation from an arbitrary receiver surface. Int J Heat Mass Transfer 1973;16:271–80.
[40] Evans DL. On the performance of cylindrical parabolic solar concentrators with flat absorbers. Sol Energy 1977;19:379–85.
[41] Nicolas RO, Duran JC. Generalization of the two-dimensional optical analysis of cylindrical concentrators. Sol Energy 1980;25:21–31.
[42] James A, Harris WSD. Focal plane flux distribution produced by solar concentrating reflectors. Sol Energy 1981;27:403–11.
[43] Rabl A. Active solar collectors and their applications. New York (USA): Oxford University Press; 1985.
[44] Jeter SM. The distribution of concentrated solar radiation in paraboloidal collectors. J Sol Energy Eng 1986;108:219–25.
[45] Jeter SM. Calculation of the concentrated flux density distribution in parabolic trough collectors by a semifinite formulation. Sol Energy 1986;37(5):335–45.
[46] Jeter SM. Analytical determination of the optical performance of practical parabolic trough collectors from design data. Sol Energy 1987;39(1):11–21.
[47] Hegazy AS, EL-Kassaby MM, Hassab MA. Prediction of concentration distribution in parabolic trough solar collectors. Int J Sol Energy 1994;16:121–35.
[48] Rabl A, Bendt P, Gaul HW. Optimization of parabolic trough solar collectors. Sol Energy 1982;29:407–17.
[49] Huang WD, Hu P, Chen ZS. Performance simulation of a parabolic trough solar collector. Sol Energy 2012;86:746–55.
[50] Ho CK. Software and codes for analysis of concentrated solar power technologies. SANDIA REPORT, SAND 2008-8053, unlimited release, printed December 2008.
[51] Garcia P, Ferriere A, Bezian JJ. Codes for solar flux calculation dedicated to central receiver system applications: a comparative review. Sol Energy 2008;82:189–97.
[52] Shuai Y, Xia XL, Tan HP. Radiation performance of dish solar concentrator/cavity receiver systems. Sol Energy 2008;82:13–21.
[53] Wang FQ, Shuai Y, Yuan Y, Liu B. Effects of material selection on the thermal stresses of tube receiver under concentrated solar irradiation. Mater Des 2012;33:284–91.
[54] Cui FQ, He YL, Cheng ZD, Li D, Tao YB. Numerical simulations of the solar transmission process for a pressurized volumetric receiver. Energy 2012;46(1):618–28.
[55] Cheng ZD, He YL, Cui FQ. Numerical investigations on coupled heat transfer and synthetical performance of a pressurized volumetric receiver with MCRT-FVM method. Appl Therm Eng 2013;50:1044–54.
[56] Cheng ZD, He YL, Cui FQ. A new modelling method and unified code with MCRT for concentrating solar collectors and its applications. Appl Energy 2013;101:686–98.
[57] Wang FQ, Lin RY, Liu B, Tan HP, Shuai Y. Optical efficiency analysis of cylindrical cavity receiver with bottom surface convex. Sol Energy 2013;90:195–204.
[58] Cooper T, Steinfeld A. Derivation of the angular dispersion error distribution of mirror surfaces for MCRT applications. J Sol Energy Eng 2011;133:044501-1–1-8.
[59] Aldali Y, Muneer T, Henderson D. Solar absorber tube analysis: thermal simulation using CFD. Int J Low-Carbon Technol 2011:1–6.
[60] Roesle M, Coskun V, Steinfeld A. Numerical analysis of heat loss from a parabolic trough absorber tube with active vacuum system. J Sol Energy Eng 2011;133:031015-1–5-5.
[61] Muñoz J, Abánades A. Analysis of internal helically finned tubes for parabolic trough design by CFD tools. Appl Energy 2011;88:4139–49.
[62] Roldán MI, Valenzuela L, Zarza E. Thermal analysis of solar receiver pipes with superheated steam. Appl Energy 2013;103:73–84.
[63] Huang WD, Huang FR, Hu P, Chen ZS. Prediction and optimization of the performance of parabolic solar dish concentrator with sphere receiver using analytical function. Renew Energy 2013;53:18–26.
[64] Prahl SA, Keijzer M, Jacques SL, Welch AJ. A Monte Carlo model of light propagation in tissue. Dosim Laser Radiat Med Biol 1989;5:102–11.
[65] Howell JR, Bannerot RB, Vliet CC. Solar-thermal energy systems analysis and design. McGraw-Hill Book Company; 1982.
[66] Geyer M, Lüpfert E, Osuna R, Esteban A, Schiel W, Schweitzer A, et al. EUROTROUGH – parabolic trough collector developed for cost efficient solar power generation. In: 11th Int symposium on concentrating solar power and chemical energy technologies, Zurich, Switzerland, September 4–6, 2002.
[67] Gossamer and 3M. Large aperture trough (LAT) 73 – engineered by Gossamer and 3M, sales data sheet; 2013. <www.3M.com/solar>.
[68] Schott. Schott PTR70 receiver – setting the benchmark. Sales data brochure; 2013. <http://www.us.schott.com/csp/english/schott-solar-ptr-70-receivers.html>.
[69] Siemens. The unrivaled benchmark in solar receiver efficiency. Sales data brochure; 2013. <http://www.energy.siemens.com/hq/en/renewable-energy/solar-power/concentrated-solar-power/products/receivers.htm>.